Available online at www.sciencedirect.com
ScienceDirect
International Journal of Heat and Mass Transfer 51 (2008) 2389–2397
International Journal of HEAT and MASS TRANSFER
www.elsevier.com/locate/ijhmt

A new structural model of effective thermal conductivity for heterogeneous materials with co-continuous phases

Jianfeng Wang [a,*], James K. Carson [b], Mike F. North [c], Donald J. Cleland [a]

[a] Institute of Technology and Engineering, Massey University, Private Bag 11-222, Palmerston North, New Zealand
[b] Department of Engineering, University of Waikato, Private Bag 3105, Hamilton, New Zealand
[c] AgResearch Ltd., Private Bag 3123, Hamilton, New Zealand

Received 15 January 2007; received in revised form 10 August 2007
Available online 22 October 2007

Abstract

A new structural model for a heterogeneous material with multiple continuous phases is proposed. The corresponding equation for effective thermal conductivity was derived using three methods. The new model is substantially different from the conventional five fundamental structural models (Series, Parallel, two forms of Maxwell–Eucken, Effective Medium Theory). The model has two applications. First, as a new fundamental structural model to produce composite models using the combinatory rules previously proposed by J.F. Wang, J.K. Carson, M.F. North, D. J. Cleland, A new approach to modelling the effective thermal conductivity of heterogeneous materials, International Journal of Heat and Mass Transfer, 49 (17–18) (2006) 3075–3083. Second, to narrow the bounds of the effective thermal conductivity for heterogeneous materials where the physical structure can be characterised into general classes.

Keywords: Co-continuous; Effective thermal conductivity; Bounds; Isotropic; Anisotropic; Heterogeneous material

1. Introduction

Heterogeneous or composite solid materials are widely used in heat transfer processes and thermal management equipment. Effective thermal conductivity is one of the key thermophysical properties used for quantifying the thermal behaviour of heterogeneous materials. Carson [1,2] reviewed the relevant modelling approaches. A heterogeneous material's effective thermal conductivity is strongly affected by its composition and structure. For materials with simple physical structures, the effective thermal conductivity can be modelled using existing fundamental structural models like those given in Table 1 (for two-phase materials). However, for some materials with complicated physical structures, these basic models are not appropriate. An alternative method is to use empirical models which are generally obtained by modifying simple models such as those listed in Table 1. Another common way of estimating effective thermal conductivity for heterogeneous materials with known microstructures is to make rigorous numerical simulations using the finite difference method, the finite element method, or other numerical techniques [3–5]. However, analytical models are preferred over numerical models in many applications due to their physical basis, rapid and low cost of calculation, and reasonable accuracy even when microstructure is uncertain. Recently, Wang et al. [6] proposed a new procedure for modelling complex materials as composites of five basic structural models (Series, Parallel, two forms of Maxwell–Eucken, Effective Medium Theory) using simple combinatory rules. The advantage of this method is that 26 new 'composite' models can be produced from these five basic models and each has a distinct physical basis. But this method is limited to the number of the basic structural models used for combination. In other words, the basic models adopted must include all of the heterogeneous

* Corresponding author. Tel.: +64 6 356 9099x7284; fax: +64 6 350 5604.
E-mail address: J.F.Wang@massey.ac.nz (J. Wang).

0017-9310/$ - see front matter © 2007 Elsevier Ltd. All rights reserved.
doi:10.1016/j.ijheatmasstransfer.2007.08.028

Nomenclature

A,B,C	different phases/components constituting a material
BN	boron nitride
c_1,c_2	constants in Eq. (19)
CC	co-continuous model
EG	ethylene glycol
EMT	effective medium theory
f	volume fraction of a phase
H	temperature gradient (K m^{-1})
k	thermal conductivity of a phase (W m^{-1} K^{-1})
K	effective thermal conductivity of a heterogeneous material (W m^{-1} K^{-1})
ME1	Maxwell–Eucken model with the first phase as the continuous phase
ME2	Maxwell–Eucken model with the second phase as the continuous phase
N	number of phases
P	depolarisation factor
PB	polybenzoxazine
PS	polystyrene
q	heat flux (W m^{-2})
r	radial distance (m)
R	radius of sphere (m)
SS	stainless steel
v	volume fraction of a phase

Greek symbols

ϕ	elevation direction
θ	azimuthal direction

Subscripts

c	continuous phase
e	effective
i	ith phase
j	jth principal axis
p	parallel model
s	series model

material's basic structures that can contribute to the overall physical structure and behaviour of the material.

Both the authors' previous work [1,2,6] and several other studies [11–14] on effective thermal conductivity have demonstrated the importance of these five fundamental structural models on theoretical analyses and for developing more complex theoretical and empirical models. In particular, an important analysis is to define thermal conductivity bounds for certain classes of physical structure. Of the five fundamental structural models shown in Table 1, the series and parallel models represent a laminate (layered) structure of the phases. The other three models, two forms of ME (Maxwell–Eucken) [7,8] and EMT (Effective Media Theory)[9,10], are based on the phases being continuous and/or dispersed: the ME model represents one continuous phase and one or more dispersed phases, and EMT by all phases being mutually dispersed. The authors conjecture the existence of a new fundamental model that is characterised by all phases being continuous. This paper will derive a co-continuous structural model using three techniques, and will show its application for improving the prediction of effective thermal conductivity of heterogeneous materials.

2. Derivations of co-continuous structural model

2.1. Mathematical deduction

Brailsford and Major [12] proposed a procedure for mathematically deriving the EMT model by using the ME model for an isotropic material with two dispersed phases and one continuous phase. Taking a similar approach, we assume an isotropic material with two continuous phases A and B and one dispersed phase C. As shown in Fig. 1, the dispersed phase C is assumed to be split between the two continuous phases with a volume fraction f_c dispersed in phase A and a volume fraction $(1-f_c)$ dispersed in phase B. Using the ME model, the effective thermal conductivity of the two sub-assemblies can be expressed by:

$$K_{e1} = \frac{k_A v_A + k_c f_c v_c \frac{3k_A}{2k_A+k_c}}{v_A + f_c v_c \frac{3k_A}{2k_A+k_c}} \tag{1}$$

$$K_{e2} = \frac{k_v v_B + k_c (1-f_c) v_c \frac{3k_B}{2k_B+k_c}}{v_B + (1-f_c) v_c \frac{3k_B}{2k_B+k_c}} \tag{2}$$

Assuming a value of f_c so that the effective thermal conductivity of the overall material and the sub-assemblies are identical means that:

$$K_e = K_{e1} = K_{e2} \tag{3}$$

Also, the summation of the volume fractions for the three phases is:

$$v_A + v_B + v_C = 1 \tag{4}$$

Solving Eqs. (1)–(4) gives:

$$K_e = \frac{k_A v_A \frac{3k_B}{2k_B+k_c} + k_B v_B \frac{3k_A}{2k_A+k_c} + k_C v_C \frac{3k_A}{2k_A+k_c}\frac{3k_B}{2k_B+k_c}}{v_A \frac{3k_B}{2k_B+k_c} + v_B \frac{3k_A}{2k_A+k_c} + v_C \frac{3k_A}{2k_A+k_c}\frac{3k_B}{2k_B+k_c}} \tag{5}$$

which can be rewritten as:

$$K_e = \frac{k_A v_A \frac{2k_A+k_C}{3k_A} + k_B v_B \frac{2k_B+k_C}{3k_B} + k_C v_C}{v_A \frac{2k_A+k_C}{3k_A} + v_B \frac{2k_B+k_C}{3k_B} + v_C} \tag{6}$$

Eqs. (5) or (6) gives the effective thermal conductivity of a three-phase material assuming phase C is dispersed. Phase

Table 1
The five fundamental structural effective thermal conductivity models for two phase materials

Model	Structure schematic	Effective thermal conductivity equation	Ref.
Parallel model	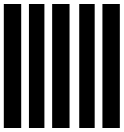	$K = v_1k_1 + v_2k_2$	
Maxwell–Eucken 1 (ME1) (k_1 = continuous phase, k_2 = dispersed phase)	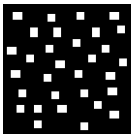	$K = \dfrac{k_1v_1 + k_2v_2\dfrac{3k_1}{2k_1+k_2}}{v_1 + v_2\dfrac{3k_1}{2k_1+k_2}}$	[7,8]
EMT model		$v_1\dfrac{k_1-K}{k_1+2K} + v_2\dfrac{k_2-K}{k_2+2K} = 0$	[9,10]
Maxwell–Eucken 2 (ME2) (k_1 = dispersed phase, k_2 = continuous phase)	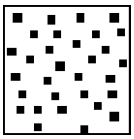	$K = \dfrac{k_2v_2 + k_1v_1\dfrac{3k_2}{2k_2+k_1}}{v_2 + v_1\dfrac{3k_2}{2k_2+k_1}}$	[7,8]
Series model	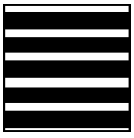	$K = \dfrac{1}{v_1/k_1 + v_2/k_2}$	

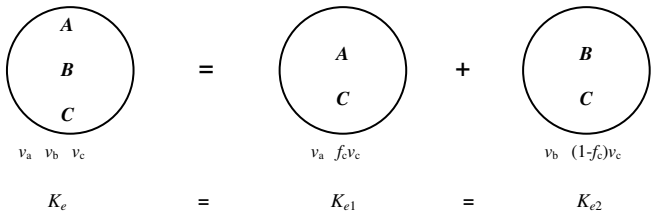

Fig. 1. A structural model with two continuous phases (A and B) and one dispersed phase (C).

C can be eliminated leaving a material comprising co-continuous phases A and B by assuming that phase C has a thermal conductivity equal to the average value of the conductivity of the two-phase structure comprising A and B only. Mathematically, this is achieved by setting $k_c = K_e$ and $v_c = 0$ in Eq. (6) and solving for K_e giving:

$$v_A\frac{(k_A - K_e)(2k_A + K_e)}{k_A} + v_B\frac{(k_B - K_e)(2k_B + K_e)}{k_B} = 0 \quad (7)$$

For a material with N co-continuous phases, a similar process can be used to derive the general model expression:

$$\sum_{i=1}^{N} v_i\frac{(k_i - K_e)(2k_i + K_e)}{k_i} = 0 \quad (8)$$

Eq. (8) can be further rewritten using the series and parallel models for a N-phase material giving:

$$K_e = \frac{K_s}{2}\left(\sqrt{1 + 8K_p/K_s} - 1\right) \quad (9)$$

where:

$$K_s = \frac{1}{\sum_{i=1}^{N}\frac{v_i}{k_i}} \quad (10)$$

$$K_p = \sum_{i=1}^{N} k_iv_i \quad (11)$$

From Eq. (9), we can see that the effective thermal conductivity of a material with co-continuous phases has a simple model solution dependent only on the series and parallel model values.

2.2. Thermal field method

A more physically rigorous method to derive the co-continuous structural model is to use the thermal field method [15]. Consider an anisotropic spherical inclusion inserted into an isotropic material with effective thermal conductivity, K_e, subjected to a uniform temperature gradient $\boldsymbol{H}$ as shown in Fig. 2a. The internal structure of the spherical inclusion is shown in Fig. 2b. It is composed of layers of the phases of the material in the inclusion. The laminate geometry means that each of the phases in the inclusion forms a co-continuous phase. The spherical shape also means that the effective thermal conductivities of the laminate spherical inclusion in the radial (r), azimuthal (θ)

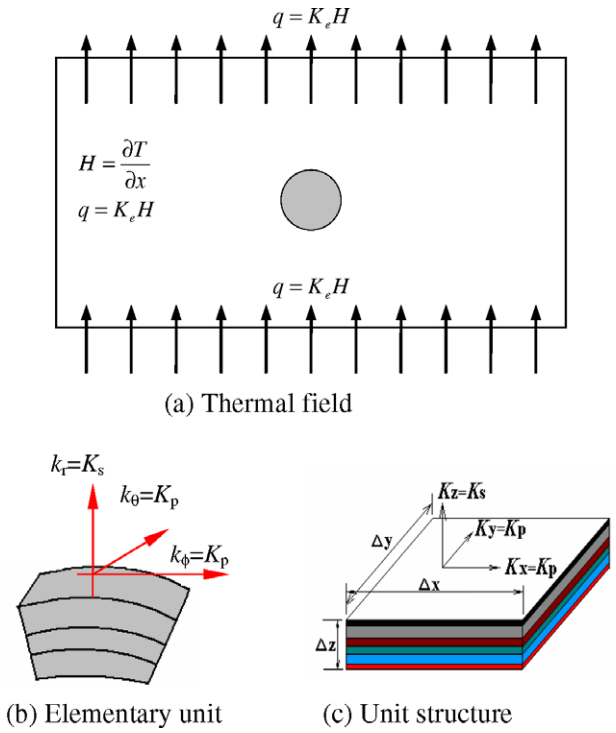

Fig. 2. A single spherical inclusion dispersed in an infinite medium with heat transfer in one direction: (a) thermal field, (b) elementary unit and (c) unit structure.

and elevation (ϕ) directions are K_s, K_p, K_p respectively (i.e. either series or parallel structures of the phases). In an isotropic material, the temperature is given by:

$$T = H \cdot r\cos\phi \tag{12}$$

To guarantee non-disturbance of the temperature field given in Eq. (12) by the spherical inclusion then:

$$T|_{r=R} = H \cdot R\cos\phi \tag{13}$$

$$q_r|_{r=R} = -K_s \frac{\partial T}{\partial r}|_{r=R} = -K_e H\cos\phi \tag{14}$$

Also for a steady state thermal field:

$$\nabla q = \mathrm{grad}(q) = 0 \tag{15}$$

Heat fluxes in the radial and elevation directions are given by:

$$q_r = -K_s \frac{\partial T}{\partial r} \tag{16}$$

$$q_\phi = -\frac{K_p}{r}\frac{\partial T}{\partial \phi} \tag{17}$$

while heat flux in the azimuthal direction is identical to the elevation direction due to symmetry. Setting the solution of Eq. (15) to be of the form:

$$T = f(r)\cos\phi \tag{18}$$

where

$$f(r) = c_1 r^{\frac{-1+(1+8K_p/K_s)^{1/2}}{2}} + c_2 r^{\frac{-1-(1+8K_p/K_s)^{1/2}}{2}} \tag{19}$$

A finite solution for temperature at $r = 0$ implies that $c_2 = 0$ in Eq. (19) and thus:

$$T = c_1 r^{\frac{-1+(1+8K_p/K_s)^{1/2}}{2}}\cos\phi \tag{20}$$

Using Eqs. (13) and (14), we can obtain the following expression for the effective thermal conductivity for the spherical inclusion in the uniform thermal field:

$$K_e = \frac{K_s}{2}\left(\sqrt{1+8K_p/K_s} - 1\right) \tag{21}$$

Having a solution for one sphere, we can insert a second, third, and so on, and fill the space left between spheres with smaller and smaller spheres all constituted as the original sphere until the limit when the space is completely filled. Hence, Eq. (21) is the final result for the effective thermal conductivity of a material only comprising co-continuous phases of the spherical inclusion. The above derivation is based on the method proposed by Schulgasser [15] except that a co-continuous structure of the sphere is assumed.

2.3. Average field approximation

The co-continuous model can also be derived using the AFA (Average Field Approximation) method [16]. The AFA is widely used for calculating the electrical conductance or resistance in electrical fields. In the method, the heterogeneous material is regarded as consisting of anisotropic grains surrounded by a homogenous medium and the effective conductivity K_e is determined self-consistently using:

$$\sum_j P_j \frac{k_j - K_e}{k_j + 2K_e} = 0 \tag{22}$$

The principal axes of the grain (x, y, z) are isotropically distributed in space. For a sphere or cube, the depolarization factors P_x, P_y, P_z all take the value of 1/3. If the conductivities in the principal axes of the grain, k_x,k_y and k_z are set to be K_p,K_p and K_s, respectively, as shown in Fig. 2c and Fig. 3a and the homogeneous medium is assumed to be continuous then:

$$\frac{1}{3}\frac{K_p - K_e}{K_p + 2K_e} + \frac{1}{3}\frac{K_p - K_e}{K_p + 2K_e} + \frac{1}{3}\frac{K_s - K_e}{K_s + 2K_e} = 0 \tag{23}$$

Solving for K_e, gives:

$$K_e = \frac{K_p}{4}\left(\sqrt{1+8K_s/K_p} + 1\right) \tag{24}$$

Eq. (22) was first obtained by Helsing and Helte [16], and Eq. (24) is a specific solution to Eq. (22) with the structural model shown in Fig. 3a.

However, the structure of the phases in the grain shown in Fig. 3a is not co-continuous. If all of the rectangular anisotropic grains are closely connected with the identical adjacent sides of other grains, the interconnected grains will become a laminated belt-shaped continuous phase with the structure shown in Fig. 3c from the overall point of view. This structure can be treated as if it formed an isotro-

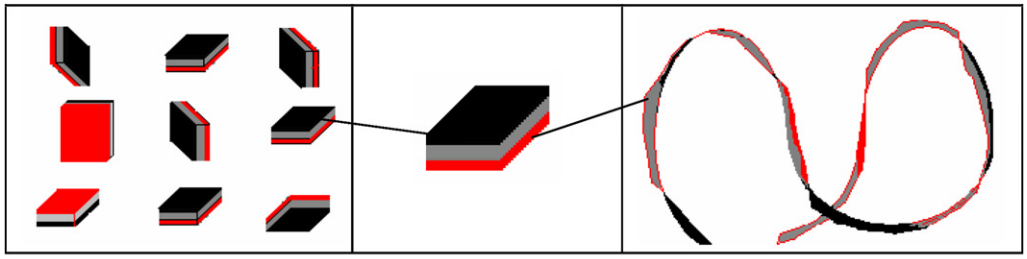

Fig. 3. Two structural models with anisotropic inclusions: (a) dispersed inclusions, (b) elementary unit and (c) continuous inclusions.

pic medium with conductivity K_e to be determined self-consistently if the principal axis conductivities are treated as being continuous. Again, taking $K_x = K_y = K_p$, and $K_z = K_s$ in Eq. (22):

$$\frac{1}{3}\frac{K_p - K_e}{K_e + 2K_p} + \frac{1}{3}\frac{K_p - K_e}{K_e + 2K_p} + \frac{1}{3}\frac{K_s - K_e}{K_e + 2K_s} = 0 \tag{25}$$

Solving Eq. (25) gives the same earlier result for the co-continuous structure:

$$K_e = \frac{K_s}{2}\left(\sqrt{1 + 8K_p/K_s} - 1\right) \tag{26}$$

Therefore, as shown in Fig. 3b, the structure of co-continuous model is anisotropic only on the micro-scale, and is effectively isotropic on the macro-scale. In addition, the co-continuous model is independent of the parallel or series model in structure although its model equation can be expressed in terms of the parallel and series model equations.

3. A new fundamental model?

The following features of the co-continuous model mean that could reasonably be classed as a 'fundamental' structural model:

(1) The co-continuous model represents an isotropic material with a distinctive structure where all phases are continuous.
(2) With the addition of the co-continuous model as a fundamental structural model, each basic model has a corresponding model with a complementary structure, i.e., the series and parallel models, the two

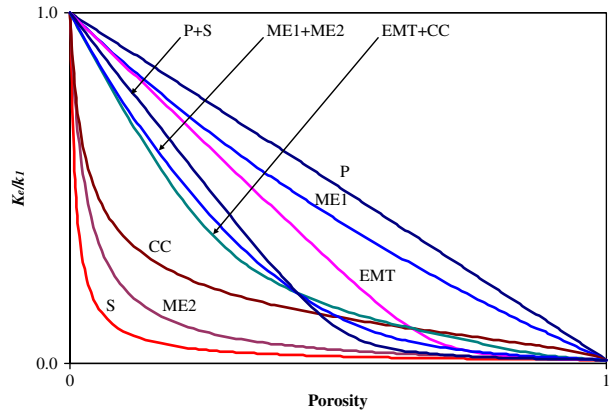

Fig. 4. Comparison of the co-continuous (CC) model with other five basic structural models and three composite models for a two-phase material with a conductivity ratio (k_1/k_2) of 100 (see [6] for the detailed calculation method for the composite models).

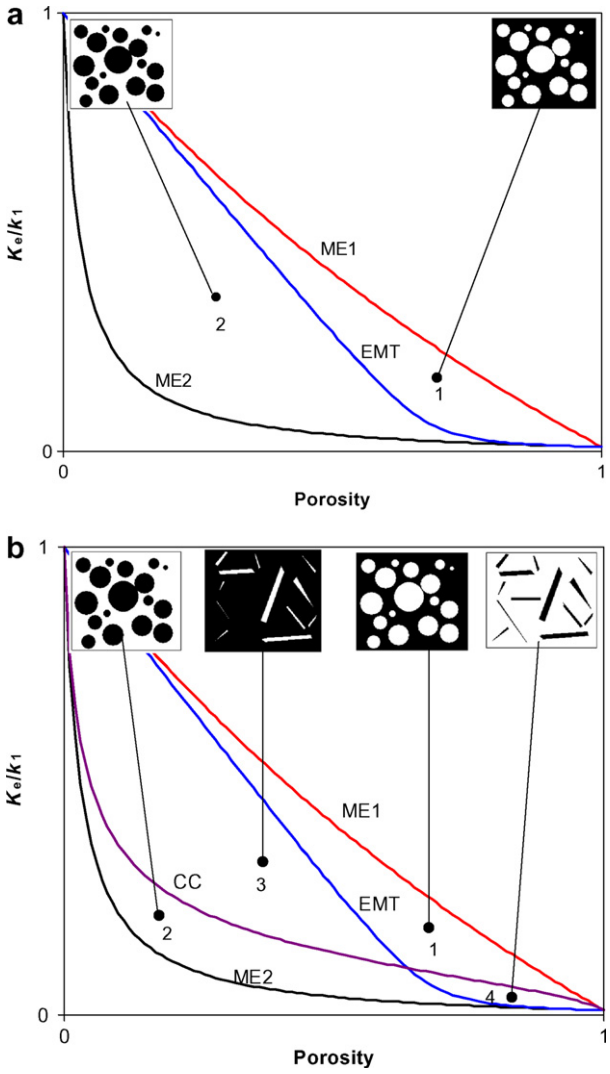

Fig. 5. Thermal conductivity bounds using the ME, EMT and CC models ($k_1 > k_2$): (a) two zone bounds [14] and (b) four zone bounds using the CC model.

ME models, and the EMT and the CC (co-continuous) models. The EMT model is characterised by all of the phases being mutually dispersed, while the CC model is characterised by all of the phases being mutually continuous.

(3) The CC model has a relation between effective conductivity and volume fraction that is very distinctive and different from the other fundamental models as shown in Fig. 4.

It should be noted that although the CC model is shown in Fig. 4 for the full range of volume fractions, not all the volume fractions will correspond to realistic physical structures. Just as the ME model, which is based on spheres dispersed randomly in a continuous matrix, does not have physical meaning above a dispersed phase volume fraction of 74% (the upper limit for the packing factor of identically sized spheres), likewise the CC structure will not necessarily have physical meaning for volume fractions close to 0 or 1.

4. Combined structural models from co-continuous model

Based on the volume fractions of each physical structure, Wang et al. [6] proposed a method to produce new structural models using combinations of the five basic structural models shown in Table 1. The model combining the two ME models was proven to represent the Levy model which has been widely used for modelling the effective thermal conductivity of meats and other porous foods [17–19]. With the five basic models in Table 1, 26 new composite structural models were obtained.

If the CC model is added as another basic model, then 31 more composite structural models can be defined, i.e. 57 composite models plus six basic models. All 63 models are independent with different structures and different model values. As shown in Fig. 4, the three composite models, P + S, ME1 + ME2, and EMT + CC have different model values though each of the three composite models represents a type of intermediate structure between the two complementary structures.

The new composite models provide a new approach to modelling the thermal conductivity of some heterogeneous materials having known compositions and unknown but fixed microstructures. For example, most biological materials like bones have relatively fixed complex structures, and their thermal conductivity can be calculated with specific combined models. The application of the combined models

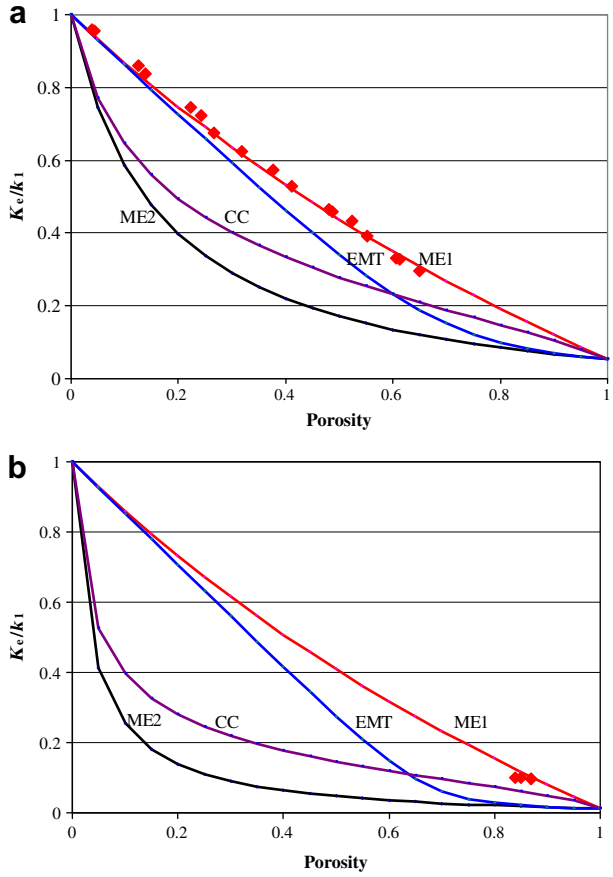

Fig. 6. Comparison between measured effective thermal conductivity and the predicted bounds given by the ME1, ME2, EMT and CC models for materials with structures in Zone 1: (a) food gel with PS balls[20] and (b) cellular ceramics with air pores [14].

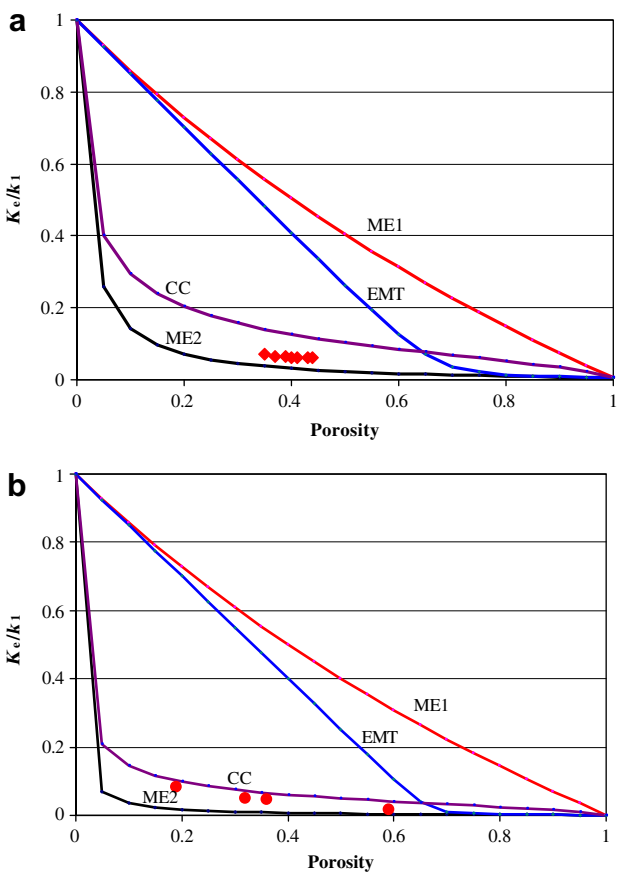

Fig. 7. Comparison between measured effective thermal conductivity [14] and the predicted bounds given by the ME1, ME2, EMT and CC models for materials with structures in Zone 2: (a) dry sand in air and (b) rock in air.

to the prediction of conductivity for a range of engineering materials and foods will be discussed in future work.

5. New bounds using the co-continuous model

For two-phase isotropic materials, the two ME models give the upper and lower bounds of the effective conductivity, known as the Hashin–Shtrikman (HS) bounds [11]. Carson et al. [14] introduced the EMT model into the HS bounds and obtained two zones with two different structures: internal porous structure and external porous structure, as shown in Fig. 5a. This approach effectively tightened the bounds for these structures to either between ME1 and EMT or between EMT and ME2.

With the addition of the CC model, as shown in Fig. 5b, the two zones within the HS bounds are divided into four zones. The different zones can be considered to comprise different phase structures and levels of connection and contact as follows.

(1) Zone 1: Internal porous structure. From the overall point of view, phase one is continuous and phase two is dispersed as separate near-spherical or cubic pores (inclusions) with some of the pores being connected. Fig. 6 shows measured effective thermal conductivity data for a food gel filled with polystyrene (PS) balls and a cellular ceramics with air pores compared with predictions for the ME1, ME2, CC and EMT models. The thermal conductivity for these heterogeneous materials appears to fall in zone 1 consistent with their known physical structure.

(2) Zone 2: External porous structure (particle bed). From the overall point of view, phase two is continuous and phase one is dispersed as separate near-spherical or cubic particles (inclusions) with some of the particles being connected or contacted. Fig. 7 shows measured effective thermal conductivity data for two samples of dry sands compared with predictions for the ME1, ME2, CC and EMT models. Again, the thermal conductivity of the sand beds appears to fall into zone 2 which is consistent with their physical structure.

(3) Zone 3: In this zone each phase is self-connected/contacted as an entity where the lumped phase 1 is surrounded by thin belt-shaped phase 2. Fig. 8 shows measured effective thermal conductivity data for solidified porous rock and sandstone, and sintered SS (stainless steel) powders and alumina powders compared with predictions for the ME1, ME2, CC

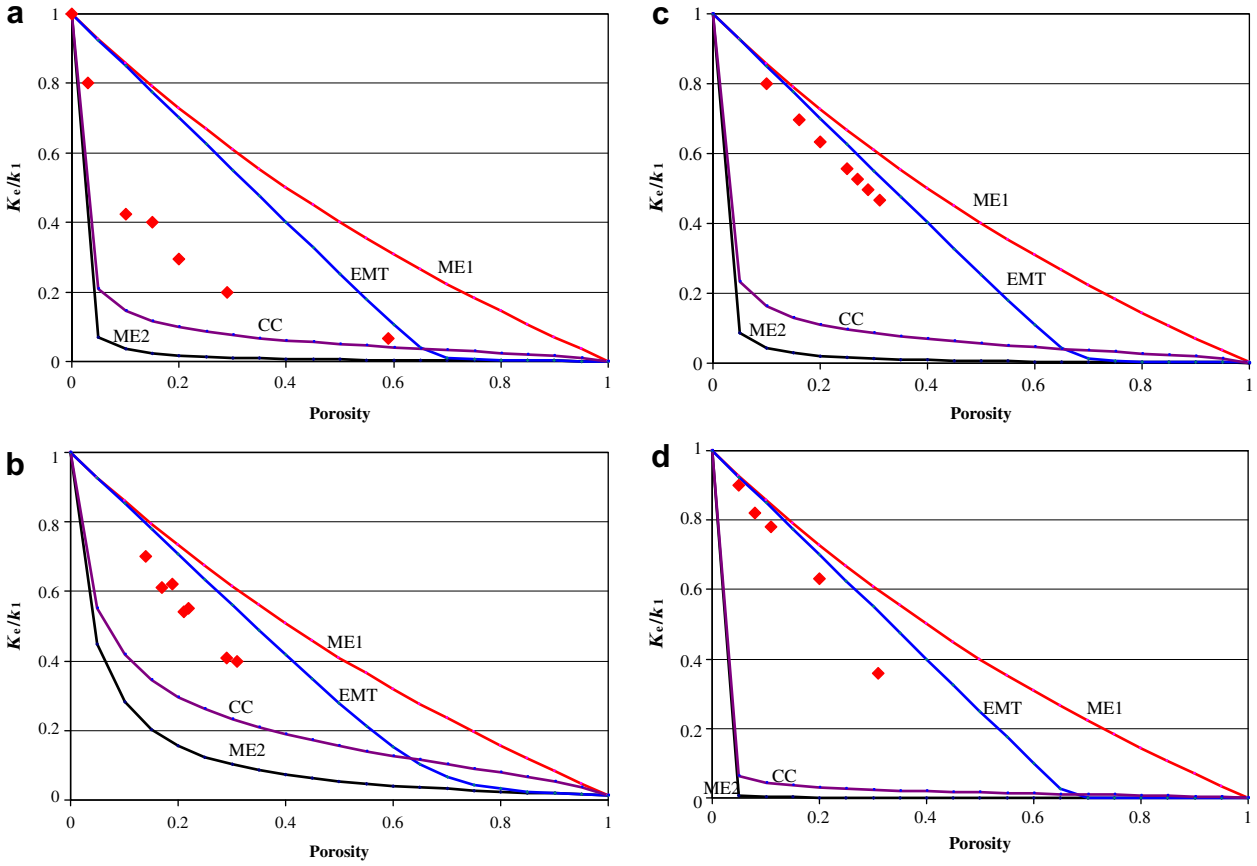

Fig. 8. Comparison between measured effective thermal conductivity and the predicted bounds given by the ME1, ME2, EMT and CC models for materials with structures in Zone 3: (a) solidified porous rock [14], (b) solidified porous sandstone [14], (c) sintered stainless steel (SS) powder in air [21] and (d) sintered aluminium powder in air [22].

and EMT models. Again, the zone 3 designation appears consistent with the structural characteristics for these materials.

(4) Zone 4: In zone 4 each phase is self-connected/contacted as an entity where the lumped phase 2 is surrounded by thin belt-shaped phase 1. Fig. 9 shows measured effective thermal conductivity data for nanotubes in oil and nanoparticles with surfactant under Brownian motion in ethylene glycol (EG) compared with predictions for the ME1, ME2, CC and EMT models. Again the data appears to fall in zone 4 consistent with their structure.

Zones 3 and 4 are both physically interconnected structures, but the dominant lumped phase is different. Therefore, the CC model does seem to provide a way to narrow the thermal conductivity bounds based on physical structure considerations. It is interesting to see from Fig. 10 that different volume fractions of platelet boron nitride (BN) filled in PS and polybenzoxazine (PB) give effective thermal conductivities in zone 3 or zone 4 which is broadly consistent with which phase is likely to be dominant.

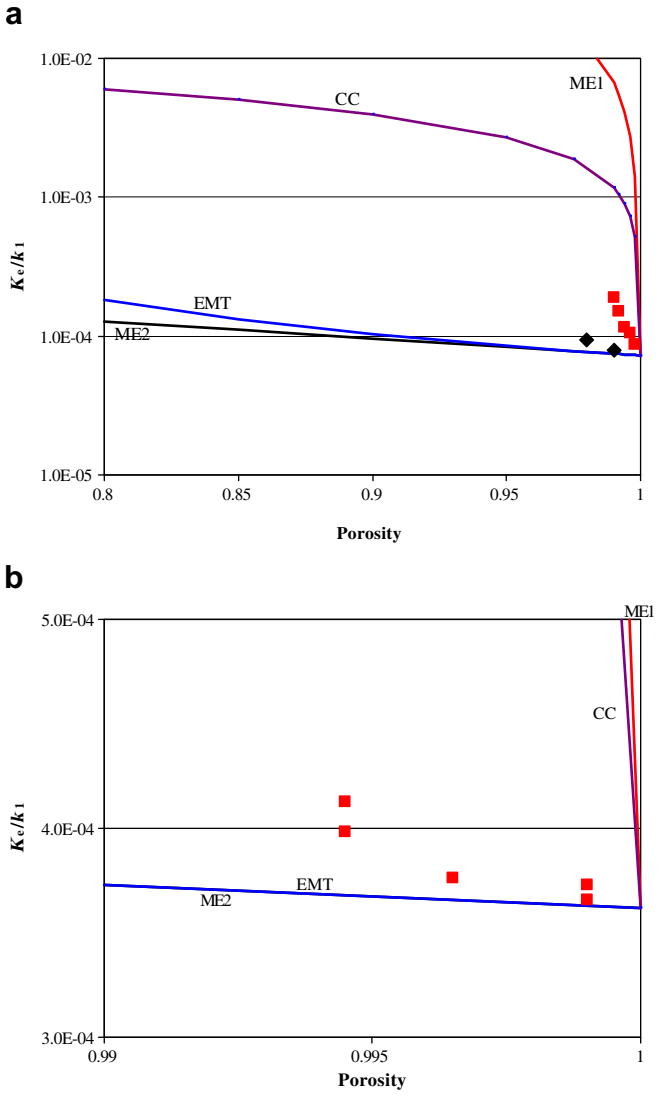

Fig. 9. Comparison between measured effective thermal conductivity and the predicted bounds given by the ME1, ME2, EMT and CC models for materials with structures in Zone 4: (a) nanotubes in oil (length/diameter > 2000, squares from [23], diamonds from [24]) (b). Nanoparticles with surfactant in ethylene glycol (EG) (Brownian motion and collision forming the connection between particles [26], $d \approx 25$ nm)[25].

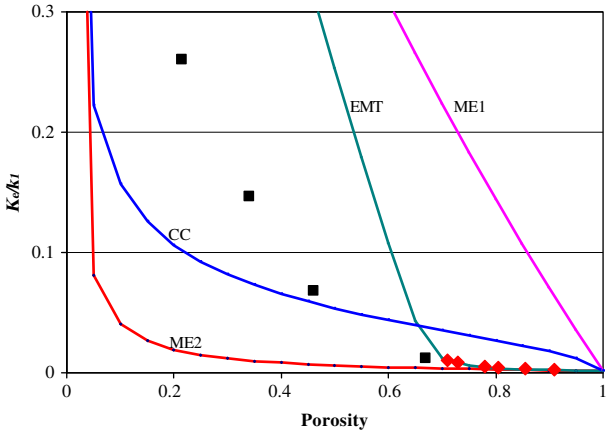

Fig. 10. Comparison between measured effective thermal conductivity for polybenzoxazine (PB) filled with platelet boron nitride (BN) (diamonds, [27]) and polystyrene (PS) filled with platelet BN (squares, [28]) and the predicted bounds given by the ME1, ME2, EMT and CC models.

6. Conclusion

This paper has derived a new structural model of effective thermal conductivity for heterogeneous materials with multiple continuous phases by using mathematical deduction, a thermal field method, and an average field approximation. This new model has a distinctive structure which is substantially different from five conventional fundamental structural models (Series, Parallel, two forms of Maxwell–Eucken, Effective Medium Theory). The new model provides more structural models using the combinatory method proposed by the authors [6]. The model also provides narrower bounds of the effective thermal conductivity within the Hashin–Shtrikman bounds for heterogeneous materials where the physical structure can be characterised.

Acknowledgement

This work was funded by the *Foundation for Research, Science & Technology* (New Zealand) as part of Objective 2 of Contract C10X0201.

References

[1] J. K Carson, Review of effective thermal conductivity models for foods, Int. J. Refrig. 29 (6) (2006) 958–967.
[2] J.K. Carson, S.J. Lovatt, D.J. Tanner, A.C. Cleland, Predicting the effective thermal conductivity of unfrozen, porous foods, J. Food Eng. 75 (3) (2006) 297–307.
[3] R. Bolot, G. Antou, G. Montavon, C. Coddet, A two-dimensional heat transfer model for thermal barrier coating average thermal

conductivity computation, Numer. Heat Transf., Part A 47 (9) (2005) 875–898.
[4] R.P.A. Rocha, M.E. Cruz, Computation of the effective conductivity of unidirectional fibrous composites with an interfacial thermal resistance, Numer. Heat Transf., Part A 39 (2) (2001) 179–203.
[5] E. Divo, A. Kassab, F. Rodriguez, Characterization of space dependent thermal conductivity with a BEM-based genetic algorithm, Numer. Heat Transf., Part A 37 (8) (2000) 845–875.
[6] J.F. Wang, J.K. Carson, M.F. North, D.J. Cleland, A new approach to modelling the effective thermal conductivity of heterogeneous materials, Int. J. Heat Mass Transf. 49 (17–18) (2006) 3075–3083.
[7] J.C. Maxwell, A Treatise on Electricity and Magnetism, third ed., Dover Publications Inc., New York, 1954 (Chapter 9).
[8] A. Eucken, Allgemeine Gesetzmäßigkeiten für das Wärmeleitvermögen verschiedener Stoffarten und Aggregatzustände, Forschung Gabiete Ingenieur 11 (1) (1940) 6–20.
[9] C.J.F. Böttcher, Theory of Electric Polarization, Elsevier, Houston, 1952 (pp. 415–420).
[10] R. Landauer, The electrical resistance of binary metallic mixtures, J. Appl. Phys. 23 (1952) 779–784.
[11] Z. Hashin, S. Shtrikman, A variational approach to the theory of the effective magnetic permeability of multiphase materials, J. Appl. Phys. 33 (1962) 3125–3131.
[12] A.D. Brailsford, K.G. Major, The thermal conductivity of aggregates of several phases including porous materials, British J. Appl. Phys. 15 (1964) 313–319.
[13] G.C.J. Bart, Thermal conduction in non homogeneous and phase change media, PhD thesis, Delft University of Technology, Netherlands, 1994.
[14] J.K. Carson, S.J. Lovatt, D.J. Tanner, A.C. Cleland, Thermal conductivity bounds for isotropic, porous materials, Int. J. Heat Mass Transf. 48 (11) (2005) 2150–2158.
[15] K. Schulgasser, Sphere assemblage model for polycrystals and symmetric materials, J. Appl. Phys. 54 (3) (1983) 380–382.
[16] J. Helsing, A. Helte, Effective conductivity of aggregates of anisotropic grains, J. Appl. Phys. 69 (6) (1991) 3583–3588.
[17] F.L. Levy, A modified Maxwell–Eucken equation for calculating the thermal conductivity of two-component solutions or mixtures, Int. J. Refrig. 4 (4) (1981) 223–225.
[18] Q.T. Pham, J. Willix, Thermal conductivity of fresh lamb meat, offal and fat in the range −40 to +30 °C: measurements and correlations, J. Food Sci. 54 (3) (1989) 508–515.
[19] B.R. Fricke, B.R. Becker, Evaluation of thermophysical property models for foods, HVAC & R Res. 7 (4) (2001) 311–329.
[20] J.K. Carson, S.J. Lovatt, D.J. Tanner, A.C. Cleland, Experimental measurements of the effective thermal conductivity of a pseudo-porous food analogue over a range of porosities and mean pore sizes, J. Food Eng. 63 (1) (2004) 87–95.
[21] J.S. Agapiou, M.F. DeVries, An experimental determination of the thermal conductivity of a 304L stainless steel powder metallurgy material, J. Heat Transf. ASME 111 (1989) 281–286.
[22] J.M. Montes, J.A. Rodriguez, E.J. Herrera, Thermal and electrical conductivities of sintered powder compacts, Powder Mettal. 46 (3) (2003) 251–256.
[23] S.U.S. Choi, Z.G. Zhang, W. Yu, Anomalous thermal conductivity enhancement in nanotube suspensions, Appl. Phys. Lett. 79 (14) (2001) 2252–2254.
[24] M.S. Liu, M.C.C. Lin, I.T. Huang, Enhancement of thermal conductivity with carbon nanotube for nanofluids, In. Commun. Heat Mass Transf. 32 (9) (2005) 1202–1210.
[25] J.A. Eastman, S.U.S. Choi, S. Li, et al., Anomalously increased effective thermal conductivities of ethylene glycol-based nanofluids containing copper nanoparticles, Appl. Phys. Lett. 78 (6) (2001) 718–720.
[26] R. Prasher, P. Bhattacharya, P.E. Phelan, Thermal conductivity of nanoscale colloidal solutions (nanofluids), Phys. Rev. Lett. 94 (2) (2005) 025901–025904.
[27] H. Ishida, S. Rimdusit, Very high thermal conductivity obtained by boron nitride-filled polybenzoxazine, Thermochim. Acta 320 (1–2) (1998) 177–186.
[28] G. Droval, P. Glouannec, J.F. Feller, et al., Simulation of electrical and thermal behavior of conductive polymer composites heating elements, J. Thermophys. Heat Transf. 19 (3) (2005) 375–381.